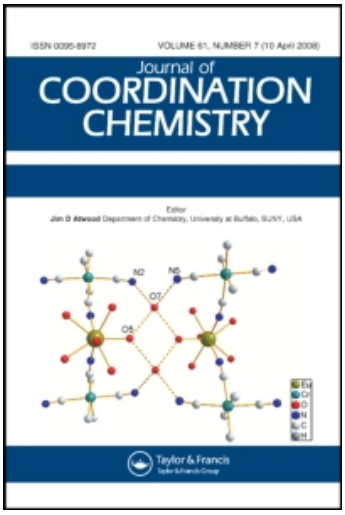

Journal of Coordination Chemistry
Publication details, including instructions for authors and subscription information:
http://www.informaworld.com/smpp/title~content=t713455674

Synthesis, characterization and antineoplastic activity of 5-chloro-2,3-dihydroxypyridine transition metal complexes

Sahar I. Mostafa[a]
[a] Faculty of Science, Chemistry Department, Mansoura University, Mansoura, Egypt

To cite this Article Mostafa, Sahar I.(2008) 'Synthesis, characterization and antineoplastic activity of 5-chloro-2,3-dihydroxypyridine transition metal complexes', Journal of Coordination Chemistry, 61: 10, 1553 — 1567
To link to this Article: DOI: 10.1080/00958970701598977
URL: http://dx.doi.org/10.1080/00958970701598977

Journal of Coordination Chemistry
Vol. 61, No. 10, 20 May 2008, 1553–1567

Taylor & Francis
Taylor & Francis Group

Synthesis, characterization and antineoplastic activity of 5-chloro-2,3-dihydroxypyridine transition metal complexes

SAHAR I. MOSTAFA*

Faculty of Science, Chemistry Department, Mansoura University, Mansoura, Egypt

(*Received 27 February 2007; in final form 27 April 2007*)

Synthetic procedures are described that allow access to *cis*-$[Mo_2O_5(cdhp)_2]^{2-}$, *cis*-$[W_2O_5(Hcdhp)_2]$, *trans*-$[OsO_2(cdhp)_2]^{2-}$, *trans*-$[UO_2(Hcdhp)_2]$, $[ReO(PPh_3)(Hcdhp)_2]X$ (X = Cl, I), $[ReO_2(cdhp)_2]^-$, $[M(PPh_3)_2(cdhp)]$, [M(bpy)(cdhp)] (M(II) = Pd, Pt), $[Ru(YPh_3)_2(Hcdhp)_2]$ (Y = P, As), $[Rh(Hcdhp)_2Cl(H_2O)]$, $[Rh(PPh_3)_2(Hcdhp)_2]ClO_4$ and $[Ir(bpy)(cdhp)Cl_2]$, where Hcdhp, cdhp are the deprotonated monoanion of 5-chloro-3-hydroxypyrid-2-one and dianion of 5-chloro-2,3-dihydroxypyridine, respectively. These complexes were characterized by their Raman, IR, ^{1}H NMR, electronic and mass spectra, conductivity, magnetic and thermal measurements. H_2cdhp, *cis*-$K_2[Mo_2O_5(cdhp)_2]$, [Pd(bpy)(cdhp)] display a significant antineoplastic activity against *Ehrlich ascites* tumor cells (EAC).

Keywords: H_2cdhp; Complexes; Spectra; EAC; Antineoplastic

1. Introduction

This report is a continuation of our research program on coordination chemistry of hydroxypyridines, reporting earlier on transition metal complexes of 1,2-dimethyl-3-hydroxy-4-pyridinone [1] and 2-amino-3-hydroxypyridine [2]. Hydroxypyridines have attracted interest in areas such as pesticide design [3–5], therapeutics, pharmacology [6–8] and as analytical reagents [9]. 2-Hydroxypyridines exist in different hydroxy-ketone forms [10]; in the solid state, 2- and 4-hydroxypyridines are predominantly in the pyridone form [11]. Hydroxypyridine, 2,3-dihydroxypyridine and substituted 2,3-hydroxylpyridines have two hydroxy groups in the *ortho* position relative to each other, and can undergo tautomerization with 2-pyridones scheme 1. The deprotonation constant (pK_a) of 2,3-dihydroxypyridine is 10.98 while that of 3-hydroxypyridine is 8.72 from involvement of the 3-hydroxy proton in a strong H-bond with the neighboring 2-carbonyl oxygen [12]. They have several coordination sites and can easily form cationic, anionic or neutral complexes, although relatively few 2,3-dihydroxypyridine complexes have been reported [12–15]. Iron(III) complexes of polydentate ligands containing the 2,3-dihydroxypyridine moiety are known [16, 17].

*Email: sihmostafa@yahoo.com

ISSN 0095-8972 print/ISSN 1029-0389 online © 2008 Taylor & Francis
DOI: 10.1080/00958970701598977

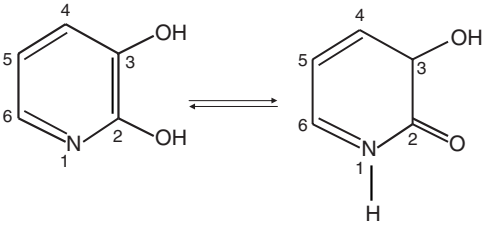

Scheme 1. 2,3-Dihydroxypyridine.

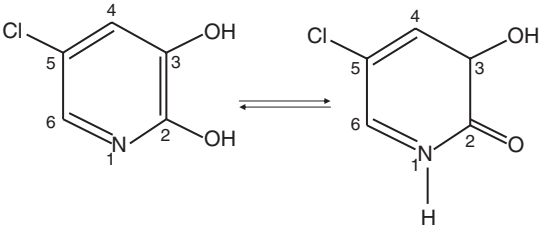

Scheme 2. 5-Chloro-2,3-dihydroxypyridine.

The X-ray crystal structure of $Fe(HL)_3$ [18] and $Al(HL)_3$ [13] are the only reports in the literature.

In this report the coordination chemistry of 5-chloro-2,3-dihydroxypyridine (H_2cdhp, scheme 2(A); 2H are the dissociable hydroxy protons) with some second and third row transition elements are explored. These complexes have been further characterized on the basis of spectral (Raman, IR, ^{1}H NMR, electronic and mass), conductivity, magnetic and thermal measurements. In addition, we report the antineoplastic activity of H_2cdhp, *cis*-$K_2[Mo_2O_5(cdhp)_2]$, [M(bpy)(cdhp)] and $[M(PPh_3)_2(cdhp)]$ (M = Pd, Pt) against *Ehrlich ascites* tumor cells (EAC).

2. Experimental

2.1. *Materials and methods*

All manipulations were performed under aerobic conditions using 5-chloro-2,3-dihydroxypyridine and all other reagents (Merck) used as received. *Trans*-$K_2[OsO_2(OH)_4]$ [19], $[ReO_2(PPh_3)_2I]$ [20], $[ReO(PPh_3)_2Cl_3]$ [21], $[M(PPh_3)_2Cl_2]$ [22, 23], $[M(bpy)Cl_2]$ (M = Pd, Pt) [24], $[Ru(PPh_3)_3Cl_2]$ [25, 26] and $[Ru(AsPh_3)_2Cl_3MeOH]$ [26] were synthesized by literature methods.

Caution! Perchlorate salts of metal complexes are potentially explosive. Only small amounts of materials should be prepared, and they should be handled with caution.

The cells of *Ehrlich ascites* (EAC) tumor were obtained from the National Cancer Institute, Cairo, Egypt. After harvesting and preparation of the cells, their total number and viability were determined by counting using Trypan blue [27].

2.2. *Instrumentation*

Microanalyses were determined by the Micro Analytical Unit of Cairo University. Magnetic moments at 25°C were recorded using a Johnson Matthey magnetic susceptibility balance with $Hg[Co(SCN)_4]$ as calibrant. Electronic spectra were recorded using a Unicam UV_{2-100} UV–vis spectrometer. IR spectra were measured as KBr discs on a Matson 5000 FT-IR spectrometer. Raman spectra were recorded as spun discs on a KBr matrix. ^1H NMR spectra were measured on a Varian Gemini WM-200 spectrometer (Laser Centre, Cairo University). Thermal analysis measurements were made in the 20–800°C range at a heating rate of 10°C min^{-1}, using α-Al_2O_3 as a reference, on a Shimadzu Thermogravimetric Analyzer TGA-50. Conductometric measurements were carried out at room temperature on a YSI Model 32 conductivity bridge. Mass spectra were recorded on a Matson MS 5988 spectrometer.

2.3. *Synthesis of complexes*

2.3.1. *Cis*-$K_2[Mo_2O_5(cdhp)_2] \cdot 2H_2O$ (1). An aqueous solution (5 cm^3) of potassium molybdate (0.23 g, 1 mmol) was added to an ethanolic solution (15 cm^3) of H_2cdhp (0.146 g, 1 mmol). The resulting yellow-orange precipitate was filtered off, washed with ethanol and diethyl ether and dried *in vacuo*. Conductivity data (10^{-3} M in DMF): $\Lambda_M = 153.0\ Ohm^{-1}\ cm^2\ mol^{-1}$.

2.3.2. *Cis*-$Y_2[Mo_2O_5(cdhp)_2]$ ($Y = PPh_4$ (2), $^nBu_4N$ (3)). Ammonium molybdate, $(NH_4)_2[MoO_4]$, (0.24 g, 1 mmol) in water (3 cm^3) was added to H_2cdhp (0.146 g, 1 mmol) in water (30 cm^3). The resulting yellow-orange solution was filtered and an aqueous solution (10 cm^3) of PPh_4Cl (0.76 g, 2 mmol) or $^nBu_4NCl$ (0.56 g, 2 mmol) was added to the filtrate. The yellow (PPh_4^+) or beige ($^nBu_4N^+$) precipitate was filtered off, washed with water and air-dried. Conductivity data (10^{-3} M in ethanol): $\Lambda_M = 46.0$ for **(2)** and 54.0 for **(3)** $Ohm^{-1}\ cm^2\ mol^{-1}$.

2.3.3. *Cis*-$[W_2O_5(Hcdhp)_2] \cdot 4H_2O$ (4). A solution of $Na_2[WO_4]$ (0.33 g, 1 mmol) in water (5 cm^3) was added to H_2cdhp (0.146 g, 1 mmol) in ethanol (15 cm^3). The pale, green-brown precipitate was filtered off, washed with ethanol and diethyl ether and dried *in vacuo*. Conductivity data (10^{-3} M in DMSO): $\Lambda_M = 4.0\ Ohm^{-1}\ cm^2\ mol^{-1}$.

2.3.4. *Trans*-$K_2[OsO_2(cdhp)_2]$ (5). $K_2[OsO_2(OH)_4]$ (0.1 g, 0.25 mmol) in water (2 cm^3) was filtered into a solution of H_2cdhp (0.073 g, 0.5 mmol) in ethanol (10 cm^3) with stirring. The resulting brown solution was left to stand for 2 h, during this time a brown complex formed. It was filtered off, washed with ethanol and diethyl ether and dried *in vacuo*. Conductivity data (10^{-3} M in DMF): $\Lambda_M = 148.0\ Ohm^{-1}\ cm^2\ mol^{-1}$.

2.3.5. *Trans*-[UO_2(Hcdhp)$_2$] · H_2O (6). *Trans*-[$UO_2(NO_3)_2$] · $6H_2O$ (0.25 g, 0.5 mmol) in methanol (10 cm^3) was added to H_2cdhp (0.146 g, 1 mmol) in methanol (20 cm^3). The red mixture was refluxed for 2 h on a steam bath. Upon reducing the volume followed by cooling, a red-brown complex separated out. It was washed with ice-cold methanol and dried *in vacuo*. Conductivity data (10^{-3} M in DMSO): $\Lambda_M = 5.0\ Ohm^{-1}\ cm^2\ mol^{-1}$.

2.3.6. [ReO(PPh_3)(Hcdhp)$_2$]Cl (7). To a stirred suspension of [ReO(PPh_3)$_2Cl_3$] (0.15 g, 0.18 mmol) in ethanol (30 cm^3) was added H_2cdhp (0.053 g, 0.36 mmol). The resulting suspension was warmed and stirred under reflux for 3 h. Pale green microcrystals were isolated, washed with ethanol and dried *in vacuo*. Conductivity data (10^{-3} M in DMSO): $\Lambda_M = 64.0\ Ohm^{-1}\ cm^2\ mol^{-1}$.

2.3.7. [ReO(PPh_3)(Hcdhp)$_2$]I (8). This complex was prepared in a similar fashion to [ReO(PPh_3)(cdhp)$_2$]Cl but with [ReO_2(PPh_3)$_2$I] in place of [ReO(PPh_3)$_2Cl_3$] and using methanol as a solvent. Conductivity data (10^{-3} M in DMSO): $\Lambda_M = 49.0\ Ohm^{-1}\ cm^2\ mol^{-1}$.

2.3.8. (PPh_4)[ReO_2(cdhp)$_2$] (9). To a stirred suspension of [ReO(PPh_3)$_2Cl_3$] (0.17 g, 0.2 mmol) in ethanol (10 cm^3) was added H_2cdhp (0.073 g, 0.5 mmol) and Et_3N (0.1 cm^3, 0.07 mmol). The resulting green suspension was stirred under reflux for 4 h and a brown solution obtained. PPh_4Cl (0.075 g, 0.2 mmol) in ethanol (5 cm^3) was added to the cold reaction mixture. Over 60 h refrigeration, a brown complex was obtained, filtered off, washed with ice-cold water and air-dried. Conductivity data (10^{-3} M in DMSO): $\Lambda_M = 28.0\ Ohm^{-1}\ cm^2\ mol^{-1}$.

2.3.9. [Pt(PPh_3)$_2$(cdhp)] (10) and [Pt(bpy)(cdhp)] (11). To a stirred suspension of H_2cdhp (0.146 g, 1 mmol) in methanol-benzene (3 : 2, V/V) (30 cm^3) was added a methanolic solution of KOH (0.11 g, 2 mmol) and [Pt(PPh_3)$_2Cl_2$] or [Pt(bpy)Cl_2] (1 mmol). The resulting suspension was stirred overnight and yellow and pale yellow complexes were obtained, respectively. These were filtered off, washed with water and methanol and air-dried. Conductivity data (10^{-3} M in DMSO): $\Lambda_M = 4.0$ for **(10)** and 2.0 for **(11)** $Ohm^{-1}\ cm^2\ mol^{-1}$.

2.3.10. [Pd(PPh_3)$_2$(cdhp)] (12) and [Pd(bpy)(cdhp)] (13). A similar procedure as for the platinum analogue was applied, [Pd(PPh_3)$_2Cl_2$] and [Pd(bpy)Cl_2] replacing their Pt(II) analogues to produce a deep-beige and brown precipitate, respectively. Conductivity data (10^{-3} M in DMSO): $\Lambda_M = 6.0$ for **(12)** and 7.0 for **(13)** $Ohm^{-1}\ cm^2\ mol^{-1}$.

2.3.11. [Ru(PPh_3)$_2$(Hcdhp)$_2$] (14) and [Ru($AsPh_3$)$_2$(Hcdhp)$_2$] (15). The complex [Ru(PPh_3)$_3Cl_2$] (0.25 g, 0.25 mmol) or [Ru($AsPh_3$)$_2Cl_3$(MeOH)] (0.21 g, 0.25 mmol) was added to methanolic solutions of H_2cdhp (0.058 g, 0.4 mmol) and Et_3N (0.05 cm^3, 0.03 mmol) was added to the reaction mixture. The reaction mixture was refluxed for 2 h during which shiny green microcrystals (PPh_3) or deep green ($AsPh_3$) product was isolated, washed with methanol and diethyl ether and dried *in vacuo*. Conductivity data (10^{-3} M in DMSO): $\Lambda_M = 4.0$ for **(14)** and 5.0 for **(15)** $Ohm^{-1}\ cm^2\ mol^{-1}$.

2.3.12. $[Rh(Hcdhp)_2Cl(H_2O)] \cdot H_2O$ (16). Hydrated rhodium trichloride (0.12 g, 0.45 mmol) was added to a solution of AcONa (0.62 g, 7.5 mmol) in water (30 cm^3) and heated gently with stirring under reflux while H_2cdhp (0.22 g, 1.5 mmol) was added. The mixture was refluxed for 6 h and a yellow-beige precipitate formed, which was removed while hot, washed with hot water and air-dried. Conductivity data (10^{-3} M in DMSO): $\Lambda_M = 6.0\ Ohm^{-1}\ cm^2\ mol^{-1}$.

2.3.13. $[Rh(PPh_3)_2(Hcdhp)_2]ClO_4$ (17). A hot ethanolic solution (15 cm^3) of H_2cdhp (0.12 g, 0.8 mmol) was added to a solution of $HClO_4$ (3 mol dm^{-3}) in water (10 cm^3) containing $RhCl_3 \cdot 3H_2O$ (0.104 g, 0.4 mmol). The resulting solution was kept under reflux for 3 h and PPh_3 (0.22 g, 0.82 mmol) in hot ethanol (10 cm^3) was added to the reaction mixture. After 1.5 h of continuing reflux, a red-brown product was isolated, filtered off while hot, washed with hot water, hot ethanol and dried *in vacuo*. Conductivity data (10^{-3} M in DMSO): $\Lambda_M = 154.0\ Ohm^{-1}\ cm^2\ mol^{-1}$.

2.3.14. $[Ir(bpy)(cdhp)Cl_2] \cdot 2H_2O$ (18). To $Na_2[IrCl_6]$ (0.113 g, 0.25 mmol) in water (5 cm^3) was added a solution of H_2cdhp (0.11 g, 0.75 mmol) and KOH (0.084 g, 1.5 mmol) in water (15 cm^3). The brown solution was kept under reflux for 2 h, then 2,2′-bipyridine (0.156 g, 1 mmol) in hot ethanol (10 cm^3) was added. The reaction mixture was refluxed for an additional 4 h and the shiny brown precipitate washed with hot water and hot ethanol and dried *in vacuo*. Conductivity data (10^{-3} M in DMSO): $\Lambda_M = 8.0\ Ohm^{-1}\ cm^2\ mol^{-1}$.

2.4. *Antineoplastic activity against Ehrlich ascites carcinoma in mice*

Ehrlich ascites tumor cells (EAC) (2×10^6 cells/mice) were implanted intrapritonial (*i.p.*). The tumor-bearing mice were divided into three groups; standard received the 5-florouracil (5-fu) for comparison, the second received H_2cdhp and its complexes and the third group is the control one (does not receive any treatment). Each group consists of seven mice. All the compounds were screened for their antitumor activity by dissolving samples in minimum amount of water, DMF or DMSO and diluting with phosphate buffered saline (PBS; pH = 7.2). H_2cdhp and *cis*-$K_2[Mo_2O_5(cdhp)_2]$, [M(bpy)(cdhp)] and $[M(PPh_3)_2(cdhp)]$ (M = Pd, Pt) complexes were injected (100 ppm solution) daily *i.p.* from the second day of incubation. The control group was treated with the same volume of 0.9% sodium chloride solution while the standard one by 5-florouracil (5-fu) [28]. All the treatments started 24 h after inoculation for 45 days.

3. Results and discussion

3.1. *Synthesis of complexes*

Hydroxypyridines undergo tautomerization with pyridones with equilibrium favoring the pyridine isomer for 2- and 4-hydroxypyridines [29]. This may make the electron-withdrawing effect of the oxygen more pronounced in the coordinated ligand and thus

further stabilize back-bonding [11]. In basic solution, this tautomerization is less favorable [11].

The Experimental Section lists new complexes of 5-chloro-2,3-dihydroxypyridine. Elemental analyses table 1 of the isolated complexes agree with the assigned formula. The oxo-molybdenum complexes *cis*-$[Mo_2O_5(cdhp)_2]^{2-}$ were prepared by reaction of H_2cdhp with $[MoO_4]^{2-}$; similar reaction using *trans*-$K_2[OsO_2(OH)_4]$ gave $K_2[OsO_2(cdhp)_2]$, while using $Na_2[WO_4]$ produced *cis*-$[W_2O_5(Hcdhp)_2]$. *Trans*-$[UO_2(Hcdhp)_2]$ was obtained by the reaction of uranyl nitrate and H_2cdhp in methanol. The $[M(PPh_3)_2(cdhp)]$ and $[M(bpy)(cdhp)]$ (M = Pd, Pt) were made from $[M(PPh_3)_2Cl_2]$ and $[M(bpy)Cl_2]$ and H_2cdhp in benzene-methanol in the presence of aqueous base. The complexes $[ReO(PPh_3)(Hcdhp)_2]X$ (X = Cl, I) were made from H_2cdhp and $[ReO(PPh_3)_2Cl_3]$ or $[ReO_2(PPh_3)_2I]$ in ethanol or methanol, respectively, while $[ReO_2(cdhp)_2]^-$ was made from $[ReO(PPh_3)_2Cl_3]$ in the presence of Et_3N in ethanol. The ruthenium complexes were made from $[Ru(PPh_3)_3Cl_2]$ or $[Ru(AsPh_3)_2Cl_3MeOH]$ and H_2cdhp in basic methanol to yield $[Ru(YPh_3)_2(Hcdhp)_2]$ (Y = P or As). $[Rh(Hcdhp)_2Cl(H_2O)]$ was obtained from $RhCl_3 \cdot 3H_2O$ and H_2cdhp under aqueous basic conditions. $[Rh(PPh_3)_2(Hcdhp)_2]ClO_4$ was prepared by the reaction of hydrated $RhCl_3$ with H_2cdhp in the presence of PPh_3 and $HClO_4$ in ethanol. Finally, the complex $[Ir(bpy)(cdhp)Cl_2]$ was obtained by refluxing $Na_2[IrCl_6]$ and the ligand in aqueous base in the presence of bpy. The sequence of reagent addition in most procedures is critical.

The complexes are microcrystalline or powder-like, stable in normal laboratory atmosphere and soluble in water (Mo, Os), DMF and DMSO. I had hoped to structurally characterize one of the complexes by single X-ray crystallography, but was thwarted on numerous occasions by very small crystal dimensions. Thus, the characterizations of the complexes were based on physical and spectroscopic techniques.

3.2. *Vibration spectra*

The characteristic Raman and IR bands observed and vibration assignments of 5-chloro-2,3-dihydroxypyridine (H_2cdhp) and its reported complexes are detailed in table 1. The IR spectra of some dihydroxypyridines show their existence in different hydroxy-ketone forms [1] scheme 1. In the solid state, H_2cdhp is predominantly in the pyridone form (form B, scheme 2) [10]. There are characteristic vibration bands of ν(NH) and ν(C=O) at 3240 and 1675 cm^{-1}, respectively [10, 11], and the in-plane β(NH) band at 1603 cm^{-1}. The broad ν(OH) absorption at 3265 cm^{-1} arises from strong intra and intermolecular hydrogen-bonding of the free ligand [11, 30].

In spectra of $[W_2O_5(Hcdhp)_2]$, $[UO_2(Hcdhp)_2] \cdot H_2O$, $[Rh(Hcdhp)_2Cl(H_2O)]$, $[Rh(PPh_3)_2(Hcdhp)_2]ClO_4$, $[ReO(PPh_3)(Hcdhp)_2]Cl$, $[ReO(PPh_3)(Hcdhp)_2]I$, $[Ru(PPh_3)_2(Hcdhp)_2]$ and $[Ru(AsPh_3)_2(Hcdhp)_2]$ the stretching vibration ν(OH) in the free ligand is missing. The band at 1675 cm^{-1} arising from ν(C=O) in the free ligand shifts to lower wave number upon complexation. The stretching vibration ν(NH) in the free ligand remains more or less in the same position in the complexes [11]. The bands at 1613 and 1566 cm^{-1}, mixed ν(C=C) and ν(C=N) modes, also shift to lower wave numbers in the complexes [1, 31]. The band near 1240 cm^{-1} in both ligand and complexes is probably due to ν(C–O). Thus H_2cdhp is a mononegative bidentate chelate through the ketonic oxygen and the *ortho* hydroxy group (form B, scheme 2); similar

Table 1. Analysis and spectral data of H_2cdhp complexes.

	Elemental analysis (Calcd)					IR Spectral data					
	C	H	N	Cl	K	ν(NH) ν(C=O)	ν^s(C=C) ν^s(C–N)	ν^s(C–C)	ν^s(C–O)	ν_s(M–O)∨	ν_{as}(M–O)[a]
Cis-$K_2[Mo_2O_5(cdhp)_2]\cdot 2H_2O$	17.77	1.34	4.08	10.67	11.56	–		1456	1240	910	874
	(17.83)	(1.19)	(4.16)	(10.55)	(11.60)					*907*	*884*
Cis-$(PPh_4)_2[Mo_2O_5(cdhp)_2]$	56.41	3.51	2.20	5.68		–		1440	1247	928	894
	(56.27)	(3.56)	(2.26)	(5.74)						*909*	*881*
Cis-$(Bu_4N)_2[Mo_2O_5(cdhp)_2]$	48.20	7.43	5.26	6.78		–		1447	1190	905	860
	(48.33)	(7.29)	(5.37)	(6.81)						*903*	*876*
Cis-$[W_2O_5(Hcdhp)_2]\cdot 4H_2O$	14.62	1.90	3.42	8.70		3221	1605		1255	912	880
	(14.84)	(1.73)	(3.46)	(8.78)		1654	1550			*919*	*894*
Trans-$K_2[OsO_2(cdhp)_2]$	19.80	0.89	4.55	11.82	12.85	–		1445	1260		840
	(19.82)	(1.00)	(4.63)	(11.73)	(12.92)					*865*	
Trans-$[UO_2(Hcdhp)_2]\cdot H_2O$	21.70	1.11	4.90	12.66		3231	1605		1264		912
	(21.47)	(1.07)	(5.0)	(12.70)		1650	1559			*879*	
$[ReO(PPh_3)(Hcdhp)_2]Cl$	42.64	2.50	3.58	13.53		3227	1608		1235	943[b]	
	(42.60)	(2.66)	(3.55)	(13.50)		1661	1536			*960*	
$[ReO(PPh_3)(Hcdhp)_2]I$	38.31	2.34	3.16			3225	1611		1232	942[b]	
	(38.17)	(2.39)	(3.18)			1668	1530			*959*	
$(PPh_4)[ReO_2(cdhp)_2]$	49.37	2.86	3.30	8.49		–		1431	1255		
	(49.26)	(2.90)	(3.38)	(8.57)							
$[Pt(PPh_3)_2(cdhp)]$	57.00	3.77	1.60	4.06		–		1443	1250	503[b]	
	(57.04)	(3.71)	(1.62)	(4.12)							
[Pt(bpy)(cdhp)]	36.26	2.00	8.43	7.15		–		1431	1254	510[b]	392[c]
	(36.39)	(2.02)	(8.49)	(7.18)							
$[Pd(PPh_3)_2(cdhp)]$	63.62	4.21	1.69	4.62		–		1437	1249	522[b]	
	(63.57)	(4.13)	(1.81)	(4.59)							
[Pd(bpy)(cdhp)]	44.25	2.51	10.40	8.71		–		1428	1248	515[b]	411[c]
	(44.35)	(2.46)	(10.35)	(8.75)							
$[Ru(PPh_3)_2(Hcdhp)_2]$	60.44	4.02	3.18	7.90		3209	1606		1248	501[b]	
	(60.39)	(3.94)	(3.06)	(7.77)		1661	1559				
$[Ru(AsPh_3)_2(Hcdhp)_2]$	55.18	3.61	2.88	6.98		3225	1610		1258	512[b]	
	(55.08)	(3.59)	(2.79)	(7.09)		1658	1530				
$[Rh(Hcdhp)_2Cl(H_2O)]\cdot H_2O$	25.84	2.37	6.00	23.07		3203	1613		1239	520[b]	340[d]
	(25.9)	(2.16)	(6.04)	(22.98)		1652	1540				
$[Rh(PPh_3)_2(Hcdhp)_2]ClO_4$	54.18	3.76	2.64	10.40		3240	1612		1236	508[b]	
	(54.36)	(3.55)	(2.76)	(0.49)		1650	1550				
$[Ir(bpy)(cdhp)Cl_2]\cdot 2H_2O$	30.28	2.67	6.96	17.85		–		1434	1247	510[b]	332[d]
	(30.07)	(2.34)	(7.02)	(17.79)							

[a]Raman data in italics, [b]ν(M–O), [c]ν(M–N), [d]ν(M–Cl).

features have been observed for the tropolonato [32, 33], maltolato [33, 34], 3-hydroxypyridin-2-one [1, 12] and *N*-substituted-3-hydroxypyridin-2-one [35, 36] complexes.

In the other complexes, the stretching vibrations ν(NH), ν(C=O) and ν(OH) in the free ligand are missing in the complexes, indicative of deprotonation and bidentate coordination of the ligand; these features are similar to those observed for catecholato and related catecholato complexes [24, 37–39]. Coordinated catechols typically show strong bands attributed to the ring stretch of the C–C bond between the two oxygen donor atoms and the C–O stretches near 1480 and 1250 cm^{-1}, respectively [24, 38, 39]. In the halo substituted catecholato complexes the (C–C) stretching frequencies are considerably lower [40]. In the spectra of complexes, these features are supported by bands near 1435 and 1245 cm^{-1}, attributed to ν(C–C) and ν(C–O) stretches, respectively.

In $[Mo_2O_5(cdhp)_2]^{2-}$ and $[W_2O_5(Hcdhp)_2]$ the symmetric *cis*-dioxo stretches, $\nu_s(MO_2)$, are seen around 910 cm^{-1} as strong bands in the Raman, weaker in the IR, with asymmetric *cis*-dioxo stretches, $\nu_{as}(MO_2)$, strong in the IR and weaker in the Raman around 880 cm^{-1}. These complexes contain a bridging oxo-ligand [41] observed in the IR near 730 cm^{-1} assigned to $\nu_{as}(M_2O)$. Both *trans*-$[UO_2(Hcdhp)_2]\cdot H_2O$ and *trans*-$K_2[OsO_2(cdhp)_2]$ show strong IR bands at 945 and 840 cm^{-1}, respectively, not observable in the Raman spectra assigned to $\nu_{as}(MO_2)$ of *trans*-O=M=O [1, 2, 42]. Strong Raman bands observed at 879 and 865 cm^{-1}, respectively, are assigned to $\nu_s(MO_2)$; in accord with *trans* geometry these bands are very weak in the IR [2, 24, 43]. The $[ReO(PPh_3)(Hcdhp)_2]I$ and $[ReO(PPh_3)(Hcdhp)_2]Cl$ complexes show a new very strong band in both Raman (959 cm^{-1}) and IR (943 cm^{-1}) spectra, from ν(Re=O) [40, 44]. In [Pd(bpy)(cdhp)], [Pt(bpy)(cdhp)] and $[Ir(bpy)(cdhp)Cl_2]$, the band of 2,2′-biyridine at 740 cm^{-1} in the free ligand is shifted to higher frequencies in the complexes (767 cm^{-1}) [45]. Also, bands at 440 and 520 cm^{-1} are assigned to ν(M–O) and ν(M–N) stretches, respectively [46, 47]. In $[Ru(PPh_3)_2(Hcdhp)_2]$, $[Ru(AsPh_3)_2(Hcdhp)_2]$ and $[Rh(PPh_3)_2(Hcdhp)]ClO_4$, strong vibrations are observed near 750, 700 and 530 cm^{-1}, attributed to PPh_3 and $AsPh_3$ [48–50]. The spectrum of $[Rh(PPh_3)_2(Hcdhp)_2]ClO_4$ exhibits two bands at 1096 cm^{-1} (strong) and 690 cm^{-1} (medium) due to $\nu_3(F_2)$ and $\nu_4(F_2)$ of uncoordinated ClO_4^-, respectively [51, 52].

3.3. *Electronic spectra*

The electronic spectra of H_2cdhp in both nujol and ethanol show three absorption bands near 210, 240 and 305 nm [12]. The electronic spectra of the complexes in H_2O, DMF or DMSO in the 200–900 nm region contain intense bands due to ligand to metal charge transfer (LMCT) transitions and weaker bands assigned to d–d transitions [53]. Transitions below 400 nm are assigned to intra-ligand charge transfer ($n \rightarrow \pi^*$ and $\pi \rightarrow \pi^*$).

The electronic spectra of palladium(II) and platinum(II) complexes in DMSO are indicative of square-planar geometry. In the visible region of the square-planar complexes of Pd(II) and Pt(II), three spin-allowed singlet-singlet d-d transitions are predicted [54, 55]. The ground state is 1A1g and the excited states corresponding to three transitions are 1A2g, 1B1g and 1Eg in order of increasing energy. Strong charge transfer transitions interfere and prevent observation of the expected bands.

The absorption band near 365 nm is assigned to combination of charge transfer from platinum or palladium to the π^* orbital of 2,2′-bipyridine or PPh_3 and d–d bands [56, 57], while the band near 480 nm is due to a combination of ligand (π) to metal charge transfer and M(II) d–d bands [57].

The electronic spectra of the ruthenium(II) complexes show shoulders near 850 nm and intense transitions near 560 ($^1A_{1g} \rightarrow {}^1T_{1g}$), 400 ($^1A_{1g} \rightarrow {}^1T_{2g}$) and 350 (ligand ($\pi$–d$\pi$)) nm [58–60]. These features indicate a low-spin octahedral geometry around Ru(II) [60]. Similar spectral data are reported for $[Ru(PPh_3)_2LCl_2]$ and $[Ru(PPh_3)_2L_2]^+$ (L = 2-(arylazo)pyrimidines) complexes [58, 59].

The electronic spectra of the rhodium(III) complexes display bands near 600, 500 and 410 nm similar to those of other six-coordinate Rh(III) complexes, assigned to $^1A_{1g} \rightarrow {}^3T_{1g}$, $^1A_{1g} \rightarrow {}^1T_{1g}$ and $^1A_{1g} \rightarrow {}^1T_{2g}$ transitions, respectively [44, 61].

The electronic spectra of $[MoO_2]^{2+}$ (in water or ethanol) and $[WO_2]^{2+}$ (in DMSO) display bands near 465 and 350 (shoulder) nm assigned to MLCT in octahedral geometry [62, 63].

The electronic spectrum of *trans*-$[UO_2(Hcdhp)_2]$ in DMSO shows bands at 470 and 385 nm due to $\Sigma_g{}^{1+} \rightarrow {}^2\pi_u$ and $n \rightarrow \pi^*$ charge transfer, respectively [64].

3.4. *^{1}H NMR spectra*

The ^{1}H NMR spectrum of H_2cdhp in d_6-DMSO shows singlets at δ 6.88 and 7.06 ppm arising from H_4 and H_6, respectively (see scheme 2 for numbering scheme). The proton of the hydroxy group appears as a broad singlet at δ 11.89 and the NH_1 proton gives a singlet at δ 9.65 ppm. In the complexes table 2, the proton of the hydroxy group is not observed while the resonances arising from H_4 and H_6 shift to lower field [65], probably due to decrease in the electron density caused by electron withdrawal of the metal in the pyridine ring coordination centers. Similar features are observed for catecholate and 1,2-dimethyl-3-hydroxypyridin-4-one complexes [1, 24, 40]. In *cis*-$[W_2O_5(Hcdhp)_2]$, $[Ru(AsPh_3)_2(Hcdhp)_2]$, $[Rh(PPh_3)_2(Hcdhp)_2]ClO_4$, $[Rh(Hcdhp)_2Cl(H_2O)]$ and *trans*-$[UO_2(Hcdhp)_2] \cdot H_2O$, the NH_1 resonance shifts downfield confirming that

Table 2. Electronic and ^{1}H NMR spectral data of H_2cdhp and its complexes.

Compounds	Electronic spectra (nm)	^{1}H NMR Spectra (ppm)			
		H(4)	H(6)	NH(1)	OH
H_2cdhp	305, 240, 201	6.88	7.06	9.65	11.89
Cis-$K_2[Mo_2O_5(cdhp)_2] \cdot 2H_2O$	465, 348 (sh)[a]	7.07	7.26	–	–
Cis-$[W_2O_5(Hcdhp)_2] \cdot 4H_2O$	462, 350 (sh)[a]	7.06	7.23	9.70	–
Trans-$[UO_2(Hcdhp)_2]$	470, 385	7.05	7.22	9.71	–
$[Pt(PPh_3)_2(cdhp)]$	470, 352	7.12	–[b]	–	–
[Pt(bpy)(cdhp)]	477, 356	7.00	7.14	–	–
$[Pd(PPh_3)_2(cdhp)]$	480, 371	6.95	7.13	–	–
[Pd(bpy)(cdhp)]	473, 365	6.92	7.11	–	–
$[Ru(AsPh_3)_2(Hcdhp)_2]$	850 (sh)[a], 555, 348	7.01	7.13	9.69	–
		7.08	7.21	9.77	
$[Rh(Hcdhp)_2Cl(H_2O)]$	595, 510, 410	7.09	7.29	9.71	–
$[Rh(PPh_3)_2(Hcdhp)_2]^+$	600, 505, 415	6.99	7.23	9.70	–
		7.04	7.30	9.79	

[a]sh = shoulder, [b]interference of H(6) with PPh_3 proton signals.

H_2cdhp is mononegative bidentate through the ketonic oxygen and the *ortho* hydroxy group (form B, scheme 2). For the other complexes, the resonance arising from the NH_1 proton is not observed confirming coordination through two deprotonated hydroxy groups.

The ^{1}H NMR spectrum of $[Rh(Hcdhp)_2Cl(H_2O)]$ should show the presence of *fac* and *mer* isomers since Hchhp$^-$ is an unsymmetrical bidentate ligand (carbonyl and hydroxy oxygen atoms are non-equivalent). In the *fac* isomer, the Hcdhp$^-$ are equivalent while in the *mer* they are different [44, 65]; one peak is observed for the NH_1 at δ 9.71 ppm, showing the presence of pure isometrical form. Protons H_4 and H_6 giving only two resonances can be assigned in a similar manner [66].

The ^{1}H NMR spectrum of $[Rh(PPh_3)_2(Hcdhp)_2]^+$ shows two resonances for each proton (NH_1, H_4 and H_6) assigned to *cis*-PPh_3 and *cis*-Hcdhp$^-$ configuration (scheme 3) as the metal to phosphine π-donation is more effective in the *cis* stereochemistry than *trans* [67]. The PPh_3 protons appear as a bulky multiplet within 7.3–7.7 ppm. The X-ray crystal structure of $[Rh(PPh_3)_2(damo)_2]^+$ showed a *cis* geometry [67].

In the ^{1}H NMR spectrum of $[Ru(AsPh_3)_2(Hcdhp)_2]$, the bulky $AsPh_3$ has an inherent disadvantage in the *cis*-configuration due to steric crowding. There are two competing forces; the steric crowding between $AsPh_3 \cdots AsPh_3$ and π-back bonding between t_2Ru and π ($AsPh_3$, Hcdhp). The latter effect predominates in the *cis*-geometry [58].

3.5. *Mass spectra*

The mass spectra of the complexes $[Pt(PPh_3)_2(cdhp)]$, $[Pd(bpy)(cdhp)]$, $[Rh(Hcdhp)_2Cl(H_2O)]$ and $[Ir(bpy)(cdhp)Cl_2]$ are determined by FAB analysis. The mass spectrum of $[Pt(PPh_3)_2(cdhp)]$ shows fragmentation patterns corresponding to the successive degradation of the molecule. The first signal is at *m*/*e* 864 (Calcd 862.6), in agreement with the molecular ion of the complex, $[Pt(PPh_3)_2(cdhp)]^+$, with 6.6% abundance. The second and third signals represent the loss of cdhp and PPh_3 fragments, indicating stepwise ligand loss to $[Pt(PPh_3)_2]^+$ with *m*/*e* 721 (Calcd 719.1) and $[Pt(PPh_3)]^+$ with *m*/*e* 458 (Calcd 457.1), respectively [24]. The mass spectrum of [Pd(bpy)(cdhp)] shows a signal at *m*/*e* 408 (Calcd 405.9) representing the molecular ion of the complex, $[Pd(bpy)(cdhp)]^+$, with 3.2% abundance. The spectrum exhibits one more signal at *m*/*e* 264 (Calcd 262.4), which represents $[Pd(bpy)]^+$. The mass spectrum of $[Rh(Hcdhp)_2Cl(H_2O)] \cdot H_2O$ shows a signal at *m*/*e* 464 corresponding to $[Rh(Hcdhp)_2Cl(H_2O)]^+$ with 16.2% abundance. The spectrum shows signals at 410,

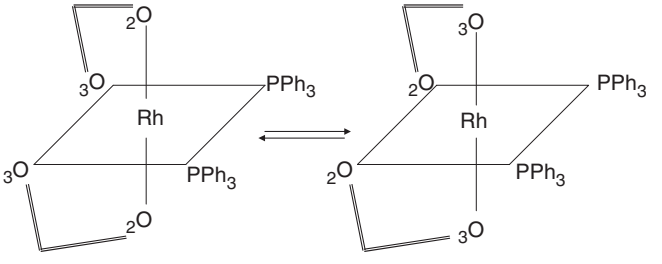

Scheme 3. Possible *cis*-configurations of $[Rh(Hcdhp)_2(PPh_3)_2]^+$.

393 and 249 corresponding to $[Rh(Hcdhp)_2(H_2O)]^+$ [68], $[Rh(Hcdhp)_2]^+$ and $[Rh(Hcdhp)]^+$ fragments, respectively. The mass spectrum of $[Ir(bpy)(cdhp)Cl_2]\cdot 2H_2O$ shows a signal at *m*/*e* 601 (Calcd 598.7) with 13.25% abundance. The fragmentation patterns indicate the stepwise ligand loss to $[Ir(bpy)(cdhp)]^+$ (494), $[Ir(bpy)]^+$ (350) [24].

3.6. *Thermal analysis*

Thermal decompositions of $[Ir(bpy)(cdhp)Cl_2]\cdot 2H_2O$, [Pd(bpy)(cdhp)], $[Rh(Hcdhp)_2Cl(H_2O)]\cdot H_2O$, $[Ru(AsPh_3)_2(Hcdhp)_2]$ and $[ReO(PPh_3)(Hcdhp)_2]Cl$ were studied using thermogravimetry (TG). The thermogram of $[Ir(bpy)(cdhp)Cl_2]\cdot 2H_2O$ shows the first step weight loss of 5.9% between 32 and 170°C, which corresponds to the release of two mol of H_2O per mol of complex (Calcd 6.0%); the relatively low temperature shows crystal lattice water [51, 61]. Another endothermic decomposition occurs between 171 and 449°C; this weight loss is attributed to loss of Cl_2 and C_5H_2NCl fragments (Calcd 30.5, Found 30.3%) [63, 69]. There are two other TG inflections in the ranges 450–509 and 510–649°C, from elimination of two halves of the bpy (Calcd 13.0, Found 13.0%) [61], leaving IrO_2 representing (Calcd 37.4, Found 37.3%). The data for [Pd(bpy)(cdhp)] show two TG inflections in the ranges 272–434 and 444–498°C. The first from release of C_5H_2NCl (Calcd 27.5, Found 27.5%) and bpy (Calcd 38.4, Found 38.5%) fragments, respectively [70], followed by the formation of PdO at 590°C (Calcd 30.2, Found 30.3%). The thermogram of $[Rh(Hcdhp)_2Cl(H_2O)]\cdot H_2O$ is characterized by steps at 41–110, 280–410, 411–490 and 491–643°C regions. The elimination of crystal lattice water (Calcd 3.9, Found 4.0%) [61], coordinated water, half Cl_2, C_5H_3OCl fragments (Calcd 36.3, Found 36.8%) [69], C_5H_3Cl species (Calcd 21.2, Found 20.9%) and N_2 (Calcd 6.0, Found 6.0%) leaving Rh_2O_3 residue at 670°C (Calcd 32.6, Found 34.1%). The TG of $[Ru(AsPh_3)_2(Hcdhp)_2]$ shows the first endothermic weight loss between 129 and 277°C, corresponding to the release of four Ph groups ($C_{24}H_{20}$) (Calcd 30.7, Found 30.2%). The second weight loss (Calcd 22.4, Found 21.9%) between 278 and 347°C is from elimination of two C_5H_3NCl fragments. The third TG inflection in the 416–516°C range may arise from release of two AsPh fragments (Calcd 30.3, Found 31.6%), followed by mixed Ru_2O_3–RuO_2 residue (21.1%). The thermogram of $[ReO(PPh_3)(Hcdhp)_2]Cl$ shows an endothermic step between 185 and 325°C, which may correspond to release of half Cl_2 and three Ph groups ($C_{18}H_{15}$) (Calcd 33.8, Found 34.0%) [69]. The second weight loss (Calcd 18.2, Found 18.5%) between 326 and 370°C may be attributed to elimination of P and C_5H_3NCl species. The third TG inflection lies in the 420–580°C range from release of O_2 and C_5H_3NCl fragments (Calcd 18.3, Found 18.8%), followed by a residue of Re-oxide (26.7%).

3.7. *Antineoplastic activity*

Reliable criteria for judging the value of any anticancer drug are prolongation of life span, improving the clinical, haematological, biochemical profile and reduction in viable tumor cell count in the host [71, 72]. It is known that available anticancer drugs inhibit the haematological and biochemical parameters (haemoglobin (Hb), red blood cell counts (RBCs) and white blood cell counts (WBCs); blood picture). The target of this study is to find a drug effective against cancer without side effects on the haematological and biochemical parameters. Schiff bases derived from substituted

o-hydroxyacetophenone-glycine (L) and their complexes [ML_2] (M = Pd, Pt) in DMF exhibit potent cytotoxic activity against *Ehrlich ascites* tumor cells [73, 74]. Also, the cytotoxicity of 2-acetylpyridine-*N*-substituted-thiosemicarbazones and 2-acetylpyrazine have been reported with their Cu(II) and Fe(II) complexes [73, 75].

In order to detect the influence of H_2cdhp and its complexes on the haematological status of EAC-bearing mice, a comparison study was made among three groups of mice from the 14th day after inoculation. The three groups are tumor-bearing mice treated with 5-fu (standard [28, 76]), H_2cdhp and its complexes and control mice. The antitumor effect of H_2cdhp, *cis*-$K_2[Mo_2O_5(cdhp)_2]$, [M(bpy)(cdhp)] and [$M(PPh_3)_2$(cdhp)] (M = Pd, Pt) shows efficacy against cancer manifested by survival, activity and reduction in the tumor size; these features were not observed for the other complexes. The haematological parameters including haemoglobin (Hb), red blood cell counts (RBCs) and white blood cell counts (WBCs) data are reported in table 3. It is clear that the haematological parameters of tumor-bearing mice treated with H_2cdhp, *cis*-$K_2[Mo_2O_5(cdhp)_2]$ and [Pd(bpy)(cdhp)] exhibits significant improvements over those treated with the standard (5-fu).

The haematological parameters are recorded for the tumor-bearing mice in the control group (Hb 7.8 g dl^{-1}; RBCs 4.7 mil mm^{-3}; WBCs 24100 mil mm^{-3}) and tumor-bearing mice treated with 5-fu (Hb 10.2 g dl^{-}; RBCs 6.0 mil mm^{-3}; WBCs 7600 mil mm^{-3}). The haematological parameters of tumor-bearing mice treated with H_2cdhp (Hb 10.8 g dl^{-1}; RBCs 6.49 mil mm^{-3}; WBCs 9840 mil mm^{-3}), *cis*-$K_2[Mo_2O_5(cdhp)_2]$ (Hb 10.7 g dl^{-1}; RBCs 6.39 mil mm^{-3}; WBCs 8200 mil mm^{-3}) and [Pd(bpy)(cdhp)] (Hb 11.4 g dl^{-1}; RBCs 6.29 mil mm^{-3}; WBCs 10150 mil mm^{-3}) are near to the normal figures.

Complexes containing cyclic nitrogen atoms display significant antitumor activity [77, 78]. Also, the presence of chloro substituent in the 5-position may increase electron withdrawing from the ring and activate the metal ion to bind the tumor DNA [79].

[M(bpy)(cdhp)] (M = Pd, Pt) complexes are more effective as antitumor agents than their PPh_3 analogues, perhaps from steric crowding of the PPh_3, preventing approach to the tumor DNA [80]. The antitumor activity of [Pd(bpy)(cdhp)] is more than that of [Pt(bpy)(cdhp)], as observed for efficacy and selectivity of Pd mono-dione complex towards A-427 lung cancer being higher than the Pt mono-dione [81].

To investigate the mechanism of action of Pd(II), Pt(II) and MoO_2(II) complexes in the binding of the tumor DNA, in a DNA viscosity assay, the complexes interacted

Table 3. Haematological and biochemical parameters.

Parameter Compound	Hb[a] (12–16 g dl^{-1})	RBCs[b] (4.0–6.0 mil mm^{-3})	HCT[c] (35.0 – 50.0%)	WBCs[d] (4000 – 11000 mm^{-3})
H_2cdhp	10.8	6.49	42.5	9840
$K_2[Mo_2O_5(cdhp)_2]$	10.7	6.39	30.3	8200
[Pd(bpy)(cdhp)]	11.4	6.29	41.9	10150
$[Pd(PPh_3)_2(cdhp)]$	9.3	5.72	26.3	22400
[Pt(bpy)(cdhp)]	8.1	4.76	21.4	13600
$[Pt(PPh_3)_2(cdhp)]$	9.9	5.93	29.3	16500
5-fu(5-florouracil)	10.2	6.0	29.9	7600
Control (0.9% NaCl)	7.8	4.72	22.2	2400

[a]Hb = hemoglobin, [b]RBCs = red blood cell counts, [c]HCT = hemato crate value, [d]WBCs = white blood cell counts values in normal mice are in parentheses.

with DNA and caused viscosity greater than the normal unbound DNA. This showed that Pd(II), Pt(II) and MoO_2(II) complexes intercalate in the DNA by making the DNA coil. The Pd(II), Pt(II) and MoO_2(II) complexes attach between base pairs, extend the DNA ladder, and probably disturb the structure of DNA so it could not replicate [81]. Also, the presence of bpy in the complexes possess a multiring planar area with nitrogen bases and hence higher hydrophobicity, which would lead to intercalation more deeply into the tumor DNA [82].

The influence of solvent in cytotoxicity of H_2cdhp, *cis*-$K_2[Mo_2O_5(cdhp)_2]$, [M(bpy)(cdhp)] and $[M(PPh_3)_2(cdhp)]$ (M = Pt, Pd) show, as expected, the water soluble H_2cdhp and *cis*-$K_2[Mo_2O_5(cdhp)_2]$ are less kidney toxic and act on DNA of the tumor by a mechanism different from water insoluble compounds [56, 79].

Regarding the tumor size, the control group tumor size was $(1.0 \times 1.2\,mm^2)$, reduced by 5-fu to $(0.6 \times 0.7\,mm^2)$ while reduced by [Pd(bpy)(cdhp)] to $(0.6 \times 0.5\,mm^2)$, indicating the efficacy of the complex.

Regarding the survival time (life span) of the three groups of the above discussed bearing-mice, the group treated with 5-fu, five out of the seven mice died after one week from treatment. The group treated with H_2cdhp (four out of seven mice died after two weeks), $K_2[Mo_2O_5(cdhp)_2]$ (two out of seven mice died after one week) and [Pd(bpy)(cdhp)] (three out of seven mice died after two weeks) while in the control group (six out of seven mice died after two weeks).

The side effects and toxicity

The side effects and toxicity of H_2cdhp, $K_2[Mo_2O_5(cdhp)_2]$ and [M(bpy)(cdhp)] (M = Pd, Pt) on the mice under study have been detected. After the first week of treatment, the mice show flu-like attack and in the third week spot dropping on the hair (alopecia). Fortunately, the solid organs have not been affected.

Details of the *in vivo* antineoplastic screens (phases II & III) will be published elsewhere.

Acknowledgements

I wish to thank Prof. F. Badria (Faculty of Pharmacy, Mansoura University, Egypt) for his assistance in the anti cancerous measurements and Dr A. Atwan (FRCSed) for the valuable discussion of this section.

References

[1] W.P. Griffith, S.I. Mostafa. *Polyhedron*, **11**, 2997 (1992).
[2] S.I. Mostafa, S.A. Abd El-Maksoud. *Monatsh. Chem.*, **129**, 455 (1998).
[3] A. Pajares, J. Gianotti, G. Stettler, J. Escalada, S. Bertolotti, S. Miskoski, F. Guerri, N. Garcia. *J. Photochem. Photobiol. A*, **153**, 101 (2002).
[4] C. Tomlin (Ed.). The Pesticide Manual, British Crop Protection Council and The Royal Society of Chemistry, UK (1994).
[5] S. Dixon, C. Wells. *J. Pestic. Sci.*, **14**, 444 (1983).
[6] H. Nakano, M. Wiesser, B. Hurt, T. Kawai, Y. Yoshida, T. Nagasawa. *Eur. J. Biochem.*, **260**, 120 (1999).
[7] M. Fukushima, H. Satake, J. Uchida, Y. Shimamoto, T. Kato, T. Takechi, H. Okabe, A. Fushioka, K. Nakano, H. Ohshimo, S. Takeda, T. Shirasaka. *Int. J. Oncol.*, **13**, 693 (1998).

[8] M. Streater, P.T. Taylor, R.C. Hider, J. Porter. *J. Med. Chem.*, **33**, 1749 (1990).
[9] B.K. Singh, C.Z. Jain, R.P. Singh. *J. Indian Chem. Soc.*, **73**, 297 (1996).
[10] H.I. Abdulla, M.F. El-Bermani. *Spectrochim. Acta*, **57**, 2659 (2001).
[11] A. Szoecsik, L. Nagy, M. Scopelliti, A. Deak, L. Pellerito, K. Hegetschweiler. *J. Organomet. Chem.*, **690**, 2280 (2005).
[12] T.V. Vovk, O.V. Kovalchukova, B.E. Zaitsev, S.B. Strashnova, V.K. Belskii, A.I. Stash. *Russ. J. Coord. Chem.*, **29**, 291 (2003).
[13] V.B. Di Marco, G.G. Bombi, A. Tapparo. *J. Chem. Soc., Dalton Trans.*, 2427 (1999).
[14] A.R. Johnson, B. O'Sullivan, K.N. Raymond. *Inorg. Chem.*, **39**, 2652 (2000).
[15] C. Chen, M. Wu, A. Yeh, T.Y. Tsai. *Inorg. Chim. Acta*, **267**, 81 (1998).
[16] G. Xiao, D. Helm, R.C. Hider, P.S. Dobbin. *Inorg. Chem.*, **34**, 1268 (1995).
[17] G. Xiao, D. Helm, R.C. Hider, B.Z. Rai. *J. Phys. Chem.*, **100**, 2345 (1996).
[18] R.C. Scarrow, P.E. Riley, K. Abu-Dari, D.L. White, K.N. Raymond. *Inorg. Chem.*, **24**, 954 (1985).
[19] J.S. Malin. *Inorg. Synth.*, **20**, 61 (1980).
[20] G.F. Ciani, G. D'Alfonso, P. Romiti, A. Sironi, M. Freni. *Inorg. Chim. Acta*, **72**, 29 (1983).
[21] N.P. Johnson, C.J. Lock, G. Wilkinson. *J. Chem. Soc.*, 1054 (1964).
[22] R.C. Cookson, D.W. Jones. *J. Chem. Soc.*, 1881 (1965).
[23] J.C. Bailar, H. Itatani. *Inorg. Chem.*, **4**, 1618 (1965).
[24] W.P. Griffith, S.I. Mostafa. *Polyhedron*, **11**, 871 (1992).
[25] R.I. Kureshy, N.H. Khan, S.H. Abdi, P. Tyer. *J. Mol. Cat. A*, **121**, 25 (1997).
[26] T.A. Stephenson, G. Wilkinson. *J. Inorg. Nucl. Chem.*, **28**, 945 (1966).
[27] K.R. Sheeji, G. Kuttan, R. Kuttan. *Amala Res. Bull.*, **17**, 73 (1997).
[28] B. Ardalan, M.D. Buscagila, P.S. Schein. *Biochem. Pharmacol.*, **27**, 2009 (1978).
[29] P. Beak. *Acc. Chem. Res.*, **10**, 186 (1977).
[30] S.I. Mostafa. *Transition Met. Chem.*, **24**, 306 (1999).
[31] S.S. Tandon, C. Chander, L.K. Thompson. *Inorg. Chim. Acta*, **300-302**, 683 (2000).
[32] W.P. Griffith, C.A. Pumphrey, A.C. Skapski. *Polyhedron*, **6**, 891 (1987).
[33] A.M. El-Hendawy, M.S. El-Shahawi. *Polyhedron*, **8**, 2813 (1989).
[34] S.J. Greaves, W.P. Griffith. *Polyhedron*, **7**, 1973 (1988).
[35] Z. Zhang, S.J. Rettig, C. Orvig. *Inorg. Chem.*, **30**, 509 (1991).
[36] W.O. Nelson, S.J. Rettig, C. Orvig. *Inorg. Chem.*, **28**, 3153 (1989).
[37] W.P. Griffith. *Transition Met. Chem.*, **18**, 250 (1993).
[38] A.M. El-Hendawy, W.P. Griffith, C.A. O'Mahoney, D.J. Williams. *Polyhedron*, **8**, 519 (1989).
[39] W.P. Griffith, A.I. Nogueira, B.C. Parkin, R.N. Sheppard, A.J. White, D.J. Williams. *J. Chem. Soc., Dalton Trans.*, 1775 (1995).
[40] C.F. Edwards, W.P. Griffith, A.J. White, D.J. Williams. *J. Chem. Soc., Dalton Trans.*, 957 (1992).
[41] W.P. Griffith, C.A. Pumphrey, T.A. Rainey. *J. Chem. Soc., Dalton Trans.*, 1125 (1986).
[42] A.M. El-Hendawy, A. El-Kourashy, M.M. Shanab. *Polyhedron*, **11**, 523 (1992).
[43] C.F. Edwards, W.P. Griffith. *Polyhedron*, **10**, 61 (1991).
[44] S.I. Mostafa. *Transition Met. Chem.*, **23**, 397 (1998).
[45] M.S. Islam, R.K. Roy, M.A. Miah. *Synth. React. Inorg. Met.-Org. Chem.*, **21**, 869 (1991).
[46] S.R. Khan, I.G. Jimenez, K.H. Whitmire, A.R. Khokhar. *Polyhedron*, **19**, 983 (2000).
[47] M.S. Ali, K.H. Whitmire, T. Toyomasa, Z.H. Siddik, A.R. Khokhar. *J. Inorg. Biochem.*, **77**, 231 (1999).
[48] K. Majumder, S. Bhattacharya. *Polyhedron*, **18**, 3669 (1999).
[49] S. Basa, I. Pal, R.J. Butcher, G. Rosair, S. Bhattacharya. *J. Chem. Sci.*, **117**, 167 (2005).
[50] R. Acharyya, F. Basuli, R.Z. Wang, T.C. Mak, S. Bhattacharya. *Inorg. Chem.*, **43**, 704 (2004).
[51] S.I. Mostafa, S.P. Perlepes, N. Hadjiliadis. *Z. Naturforsch.*, **56b**, 394 (2001).
[52] K. Nakamoto. *Infrared and Raman Spectra of Inorganic and Coordination Compounds*, 4th Edn, Wiley, New York (1986).
[53] Y.T. Li, C.W. Jan, Y.J. Zheng, D.Z. Liao. *Polyhedron*, **17**, 1423 (1998).
[54] A.B.P. Lever. *Inorganic Electronic Spectroscopy*, Elsevier, New York (1984).
[55] S.P. Perlepes, P. Jacobs, H.O. Desseyn, J.M. Tsangaris. *Spectrochim. Acta*, **43A**, 771 (1987).
[56] V.X. Jin, J.D. Ranford. *Inorg. Chim. Acta*, **304**, 38 (2000).
[57] D.K. Demertzi, J.R. Miller, N. Kourkoumelis, S.K. Hadjikakou, M.A. Demertzis. *Polyhedron*, **18**, 1005 (1999).
[58] P.K. Santra, C. Sinha, W. Sheen, F. Liao, T. Lu. *Polyhedron*, **11**, 523 (1992).
[59] P.K. Santra, C. Sinha, W. Sheen, F. Liao, T. Lu. *Polyhedron*, **20**, 599 (2001).
[60] S.I. Mostafa, A.A. El-Asmy, M.S. El-Shahawi. *Transition Met. Chem.*, **25**, 470 (2000).
[61] S.I. Mostafa, M.M. Bekheit. *Chem. Pharm. Bull. Jpn*, **48**, 266 (2000).
[62] S.I. Mostafa, S. Ikeda, B. Ohtani. *J. Mol. Catal. A*, **225**, 181 (2005).
[63] M.R. Maurya, M.N. Jayaswal, V.G. Puranik, P. Chakrabarti, S. Gopinathan, C. Gopinathan. *Polyhedron*, **16**, 3977 (1997).
[64] S.I. Mostafa, K.M. Ibrahim, N. Nawar, Z.A. Younis. *Indian J. Chem.*, **43A**, 2294 (2004).

[65] M. Calvo, A.M. Lanfredi, L. Oro, M. Pinollos, C. Tejel, A. Tiripicchio, F. Ugozzoli. *Inorg. Chem.*, **32**, 1147 (1993).
[66] S. Basu, S.M. Peng, G.H. Lee, S. Bhattacharya. *Polyhedron*, **24**, 157 (2005).
[67] M. Moszner, T. Glowiak, M. Kubiak, J.J. Ziolkowski, G. Costa, C. Tavagnacco. *Polyhedron*, **16**, 307 (1997).
[68] E. Saad, M. El-Shahawi, H. Saleh, A. El-Asmy. *Transition Met. Chem.*, **31**, 155 (2007).
[69] S.I. Mostafa, M.A. Kabil, E.M. Saad, A.A. El-Asmy. *J. Coord. Chem.*, **59**, 279 (2006).
[70] C.R. Perez, J.G. Platas, H. Lotter, L. Lezama, X. Solans, S. Dominguez, P.M. Marza, M.J. Rocio, M.S. Palacios, P. Gili. *Inorg. Chim. Acta*, **255**, 139 (1997).
[71] B.D. Clarkson, J.H. Burchenal. *Prog. Clin. Cancer*, **1**, 625 (1965).
[72] C. Oberling, M. Guerin. *Adv. Cancer Res.*, **2**, 353 (1954).
[73] W.E. Antholine, J.M. Knight, D.H. Petering. *J. Med. Chem.*, **19**, 339 (1976).
[74] O.E. Offiong, S. Martilli. *Transition Met. Chem.*, **22**, 263 (1997).
[75] I.H. Hall, K.G. Rajendram, D.X. West, A.E. Liberta. *Anticancer Drugs*, **4**, 231 (1993).
[76] K. Yoshisue, Z. Hironaga, S. Yamaguchi, A. Yamamoto, S. Nagayama, Y. Kawaguchi. *Cancer Chem. Pharm.*, **46**, 51 (2000).
[77] A. Romerosa, P. Bergamini, V. Bertolasi, A. Canella, M. Cattabriga, R. Gavioli, S. Manas, N. Mantovani, L. Pellacani. *Inorg. Chem.*, **43**, 905 (2004).
[78] S.I. Mostafa. *Transition Met. Chem.*, **32**, 769 (2007).
[79] K. Yoshisue, H. Masuda, E. Matsushima, K. Ikeda, S. Nagayama, Y. Kawaguchi. *Drug Metab. Dispos.*, **28**, 1162 (2000).
[80] R.F. Borch, M.E. Pleasents. *Proc. Natl. Acad. Sci. USA*, **76**, 6611 (1979).
[81] D. Lebwohl, R. Canerra. *Eur. J. Cancer*, **34**, 1522 (1998).
[82] X. He, L. Wang, H. Chen, L. Xu, L. Ji. *Polyhedron*, **17**, 3161 (1998).